Transient Three-Dimensional Numerical Simulation of Marangoni Flow in a Liquid Column under Microgravity

Johannes Straub, and Rudi Marek
L^{A}TT$_{U}$M, Technical University of Munich
Arcisstr. 21, D–8000 Munich 2, Germany

Abstract

The interaction of buoyancy and Marangoni flow in a vertical cylindrical floating zone of aspect ratio 1 with an adiabatic free lateral surface and isothermal top and bottom walls is studied numerically in a transient three-dimensional simulation under zero-, micro- and earth-gravity conditions. In zero-gravity, a rotationally symmetric toroidal flow pattern evolves. The flow mode and the corresponding isotherms remain qualitatively unchanged in the different gravity environments. Although natural convection itself forms a single roll, no significant distortion of the symmetric toroidal flow mode occurs, when buoyancy and surface tension-driven flows interact. Most investigations of Marangoni flow in liquid bridges focus on the flow field, while the heat transfer is less emphasized. In this study, the enhancement of steady-state heat transfer is examined for Marangoni and buoyancy convection acting in the same or in opposite direction. Finally, the dependence of the overall heat transfer rate on the strength of the thermocapillary convection is established. In a range of $1 \leq Ma \leq 10^7$ no transition from the steady thermocapillary flow to stable oscillations is observed.

Introduction

When a liquid-liquid or liquid-gas interface is exposed to a temperature gradient, a flow termed (thermal) Marangoni, surface tension-driven or thermocapillary convection is induced. These gradients give rise to variations in surface tension, and via viscous shear stresses fluid particles are set into motion. Due to the dominance of buoyancy over Marangoni convection on earth in many applications, this form of natural convection was not paid much attention to for a long time. However, with the technical feasibility of experiments on board orbiting spacecrafts and sounding rockets or in drop towers, an increased interest has been redirected towards Marangoni flows. Under micro-gravity, containerless crystal growth methods have been focused on, such as floating zone melting or Czochralski growth. Numerical simulations are a decisive tool to reduce the number of expensive space experiments, to plan and facilitate new experimental set-ups, and to foster the development of those new production techniques. On the other hand, experiments provide vital information for designing, verifying, and improving computer models. Frequently, big discrepancies between numerical predictions and experimental observations occur. Although both techniques have constantly been improved, they still have different starting-points. Every numerical simulation is based on an idealized model of a given real configuration. Inhomogeneities, geometrical peculiarities or physical mechanisms not understood yet are difficult to model, while the available computer speed and memory is another limitation. Conversely, in experiments, only a limited number of measuring points with finite resolution can be realized, the necessary devices often disturb the flow, and undesired side effects often occur. Moreover, changes, e. g. in temperature, can be brought about only in a finite time, while this is possible in no time in numerical calculations. Parameters not considerable in advance may be of decisive influence. For example, the numerical studies of Straub and Schneider [24] revealed that the smallest disalignments of an experimental set-up can influence the onset of convective motion in a fluid enormously.

All in all, numerical and experimental investigations are both indispensable and should support each other.

Marangoni convection in cylindrical floating zones has been studied both numerically [1], [2], [17], [26] and experimentally [3]–[7], [14], [16], [21] under μ- and 1-g. Chun [2] and Wilcox and Chang [26] employed a two-dimensional steady-state vorticity stream-function approach in their numerical studies, while more recently Rupp et al. [17] simulated transient Marangoni convection in a GaAs floating zone with a three-dimensional finite difference scheme. Two-dimensional steady-state methods are convenient to use due to their efficiency in memory, computing time, and costs. To make them applicable, thermofluid-dynamic problems are often simplified and reduced to two dimensions. This can be reliable for symmetrical geometries and boundary conditions, or if the third dimension is assumed to be infinitely extended. However, if the flow is actually three-dimensional, vital information is lost. In general, oscillations of the flow and temperature fields are three-dimensional and time-dependent, as shown by the numerical studies of Kirchartz [10], Mihelčić and Wingerath [13], and Rupp et al. [17] and the experimental findings of Chun and Wuest [5], Monti et al. [14], Preisser et al. [16], and Schwabe et al. [21]. Conclusions regarding oscillatory convection from two-dimensional calculations are therefore questionable. Results of two-dimensional simulations are only valid within the scope of their models. Only when two-dimensional flow modes are obtained from three-dimensional calculations, it can safely be concluded that the flow is two-dimensional, indeed.

In the vertical liquid column under consideration (Fig. 1), pure surface tension-driven convection (0-g) forms a two-dimensional axisymmetric toroidal vortex [7], [16], [21], while natural convection itself (1-g) produces a non-symmetric three-dimensional single roll [8], [18]. Varying the gravity level in our simulations, a superposition of both kinds of convection implies three-dimensional temperature and flow fields. Chun and Wuest [5], Schwabe et al. [19], and Schwabe and Scharmann [20] were the first to give experimental evidence that steady Marangoni flow becomes oscillatory and three-dimensional, after a critical Marangoni number has been exceeded. We therefore utilize a three-dimensional numerical model for our calculations.

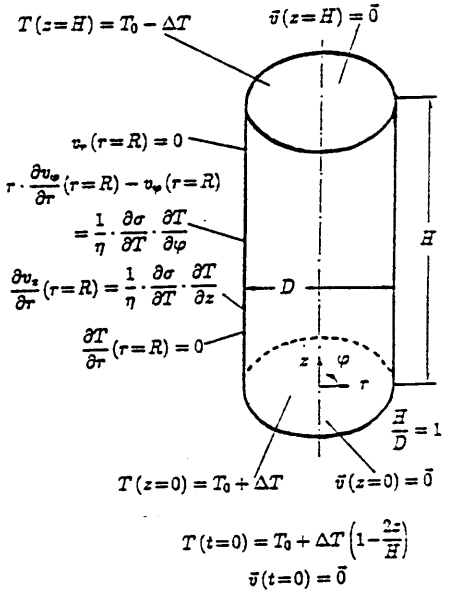

Figure 1: Geometry of the liquid column with boundary and initial conditions

Physical and Mathematical Models

The aspect ratio of a liquid bridge of diameter D and height H (Fig. 1) is defined as:

$$A = \frac{H}{D} \tag{1}$$

In the following, a floating zone with $A = 1$ is considered.

The non-slip condition applies for both rigid walls, while the lateral face is regarded as non-deformable free surface subject to the Marangoni boundary conditions. The aim of our study is to study the interaction of thermocapillary convection and buoyancy flow in a configuration as simple as possible. Therefore, the deformation of the lateral surface occurring under earth-gravity conditions is not taken into account:

$$\begin{aligned}
\vec{v}\,(r,\varphi,z=0,t) &= \vec{0} \\
\vec{v}\,(r,\varphi,z=H,t) &= \vec{0} \\
v_r\,(r=R,\varphi,z,t) &= 0 \\
r\cdot\frac{\partial v_\varphi}{\partial r}\,(r=R,\varphi,z,t) - v_\varphi\,(r=R,\varphi,z,t) &= \frac{1}{\eta}\cdot\frac{\partial\sigma}{\partial T}\cdot\frac{\partial T}{\partial\varphi} \\
\frac{\partial v_z}{\partial r}\,(r=R,\varphi,z,t) &= \frac{1}{\eta}\cdot\frac{\partial\sigma}{\partial T}\cdot\frac{\partial T}{\partial z}
\end{aligned} \tag{2}$$

Initially, the fluid between the two disks is at rest, and a hydrostatic pressure distribution is assumed:

$$\vec{v}\,(r,\varphi,z,t=0) = \vec{0} \tag{3}$$

$$p\,(r,\varphi,z,t=0) = p_0 + \varrho\cdot g_z\cdot(z_0 - z) \tag{4}$$

Concerning the thermal boundary and initial conditions, two cases are studied:

- Case 1: Initially, a linear temperature profile in axial direction due to pure heat conduction prevails, and the bottom and top disks are maintained at different temperatures constant with time:

$$\begin{aligned}
T\,(r,\varphi,z,t=0) &= T_0 + \Delta T\cdot\left(1-\frac{2z}{H}\right) \\
T\,(r,\varphi,z=0,t) &= T_0 + \Delta T \\
T\,(r,\varphi,z=H,t) &= T_0 - \Delta T
\end{aligned} \tag{5}$$

- Case 2: The system is initially isothermal, when suddenly the temperature of the bottom disk is raised by $2\,\Delta T$, while the temperature at the top wall remains T_0:

$$\begin{aligned}
T\,(r,\varphi,z,t=0) &= T_0 \\
T\,(r,\varphi,z=0,t) &= T_0 + 2\Delta T \\
T\,(r,\varphi,z=H,t) &= T_0
\end{aligned} \tag{6}$$

In both cases, the overall temperature difference is $2\,\Delta T$, and the lateral surface is supposed to be adiabatic:

$$\frac{\partial T}{\partial r}\,(r=R,\varphi,z,t)=0 \tag{7}$$

The fluid flow and the heat transfer in the liquid bridge is governed by the well-known conservation laws for mass, momentum, and energy [11]. Due to the alignment of the free surface in z-direction, axial temperature gradients are responsible for the thermocapillary flow. Therefore, the height H is used as a characteristic length to obtain the following dimensionless numbers:

$$\bullet\ \text{Rayleigh:}\quad Ra=\frac{g_z\cdot\beta_p\cdot H^3\cdot 2\,\Delta T}{\nu\cdot a} \qquad \bullet\ \text{Marangoni:}\quad Ma=\left|\frac{\partial\sigma}{\partial T}\right|\cdot\frac{2\,\Delta T\cdot H}{a\cdot\eta}$$

$$\bullet\ \text{Bond:}\quad Bo=\frac{\varrho\cdot g_z\cdot\beta_p\cdot H^2}{\left|\frac{\partial\sigma}{\partial T}\right|}=\frac{Ra}{Ma} \qquad \bullet\ \text{Nusselt (local):}\quad Nu=-\frac{\partial T}{\partial z}\cdot\frac{H}{2\,\Delta T}$$

$$\bullet\ \text{Prandtl}:\quad Pr=\frac{\nu}{a} \tag{8}$$

All fluid properties except density, which is considered in an extended Boussinesq approximation [11], are regarded as constant. A test fluid with $Pr=1.92$ is chosen.

A primitive-variable approach on a staggered grid, based on a finite control-volume hybrid difference scheme and explicit time steps, is utilized for the numerical integration of the conservation equations. The MAPLE algorithm [12] is employed for treating the pressure-velocity coupling. The cylinder axis is dealt with in the manner suggested by Schneider [18]. Further details of the computational procedure are given in [11] and [12]. The calculations were performed on a CDC Cyber 995 and a CRAY Y-MP 4/432 supercomputer.

Results

In case 1, an axisymmetric toroidal flow mode, well-known from liquid bridges on TEXUS flights [7], [16], [21], evolves under zero-gravity conditions (Fig. 2). Although the Prandtl number is not substantially greater than unity, the temperature field develops much slower with time than the flow field. At the bottom, cold fluid heats up, as it flows from the center of the disk towards the free surface thus being accelerated, while at the top wall, warm fluid is cooled down and decelerated when flowing from the outside towards the axis. This behaviour is reflected in Fig. 3 in terms of the radial development of the Nusselt number at the bottom and top disks with time. At the bottom, the Nusselt number exhibits a maximum on the axis and a minimum near the free surface, whereas this is reversed at the top. With the flow approaching its steady-state, the center of the vortex migrates towards the warm side to the lower third of the zone; its relative radial position of $r/R\approx 0.75$ agrees excellently with the observations of Preisser et al. [16] for $A=0.68$. Furthermore, the radial distribution of the axial velocity at $z=H/2$ depicted in Fig. 4 corresponds qualitatively fairly well with the findings in [16]. The basic flow mode is already established after a few seconds, as the location of $v_z=0$ is the same for $t=6$ s and $t=50$ s. The temperature at the free surface at $z=H/2$ remains almost constant with time, while the changes in the bulk are much greater (Fig. 5). This behaviour is also

reflected in Figs. 6 and 7 showing the temperature and the axial velocity distributions along the free surface. The maximum axial velocity occurs near the walls due to the steep temperature gradients.

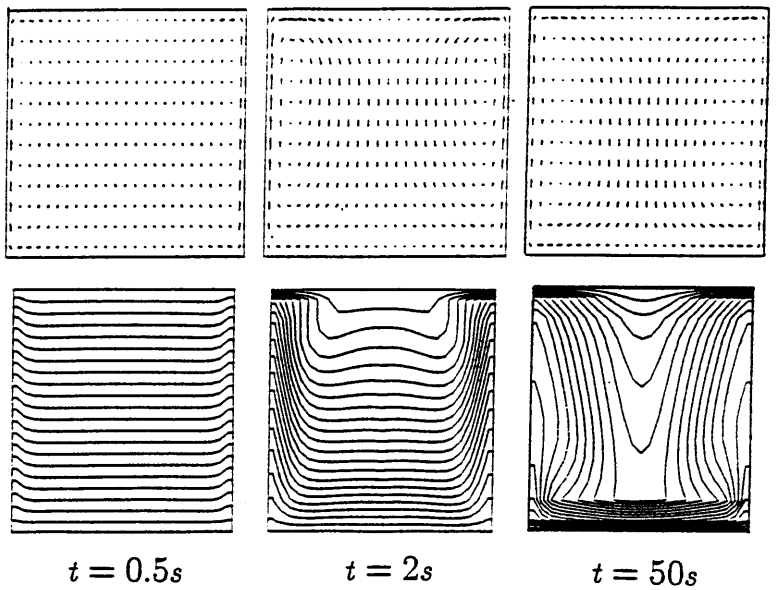

Figure 2: Transient development of velocity and temperature fields (Case 1, $Ma = 5000$, $Ra = 1.8 \cdot 10^{-36}$, $Bo = 3.6 \cdot 10^{-40}$, $Pr = 1.92$)

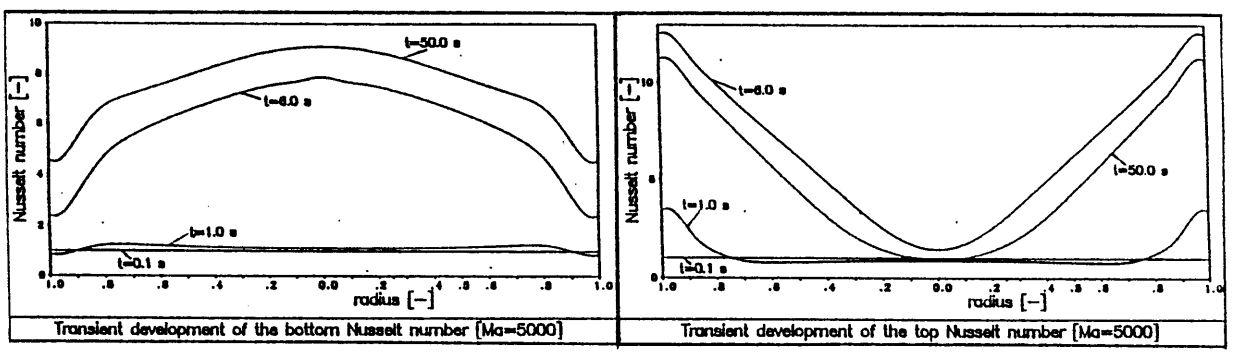

Figure 3: Nusselt numbers at the bottom and top as a function of the dimensionless radius in a cross-section $\varphi = \text{const.}$ for different times

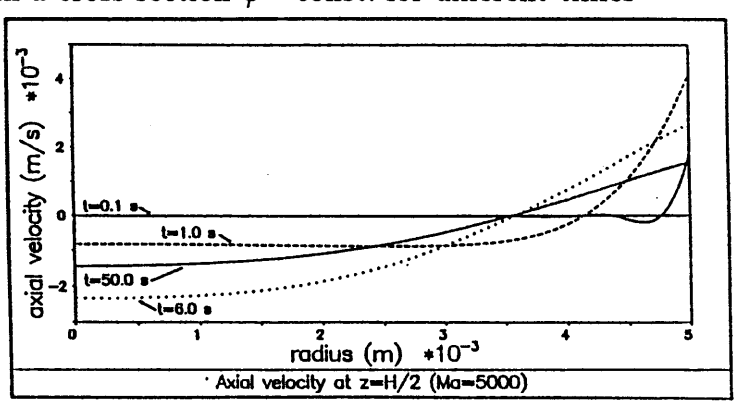

Figure 4: Transient development of the radial distribution of the axial velocity at $z = H/2$

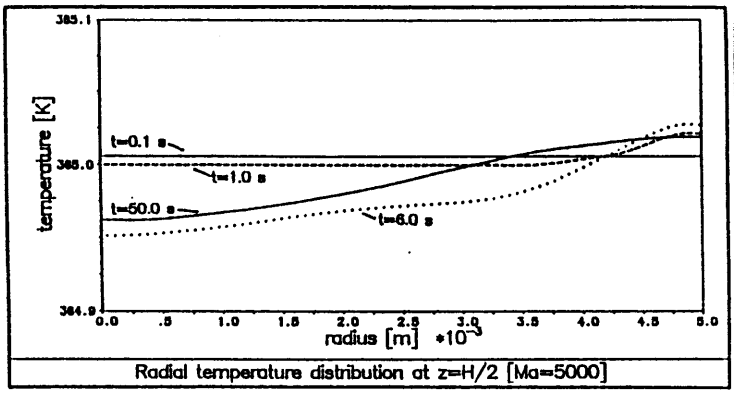

Figure 5: Transient development of the radial temperature profile at $z = H/2$

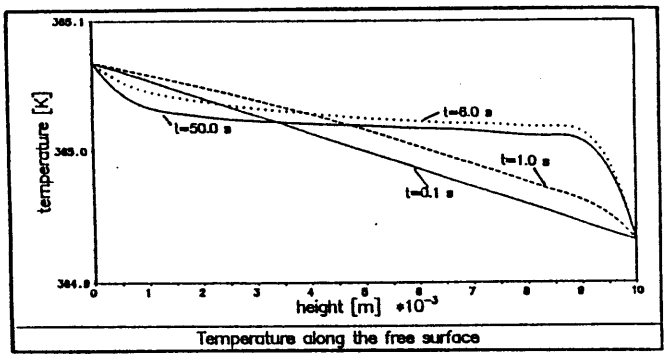

Figure 6: Transient development of the temperature along the free surface

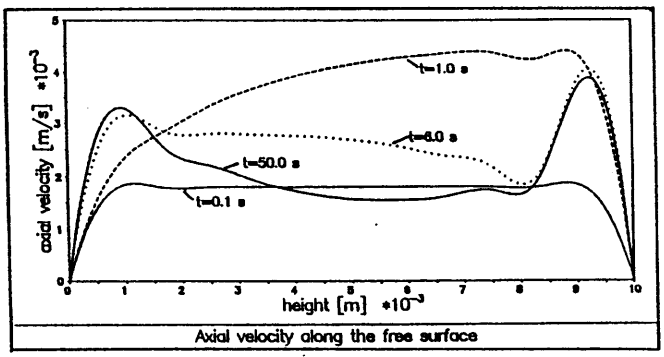

Figure 7: Transient development of the axial velocity along the free surface

For a Marangoni number of $Ma = 5000$, the steady-state heat transfer at three different gravity levels or Bond numbers, respectively, is given in terms of the Nusselt number at the warm and cold disks in Tab. 1:

Gravity level	0-g	μ-g	1-g	1-g	1-g
Remarks	pure MC	MC ↑↑ BC	MC ↑↑ BC	MC ↑↓ BC	pure BC
Bo	3.6 E-40	3.6 E-02	3.6 E00	3.6 E00	∞
Ra	1.8 E-36	1.8 E02	1.8 E04	1.8 E04	1.8 E04
Ma	5.0 E03	5.0 E03	5.0 E03	5.0 E03	0.0 E00
$\overline{Nu}$	6.922	6.928	7.44	6.29	2.65

Table 1: Integral steady-state Nusselt numbers for different gravity levels (MC=Marangoni convection, BC=buoyancy convection)

In accordance with the experiments of Schwabe et al. [21], the velocity and temperature distributions in the different gravity environments do not deviate significantly from each other. Despite the occurrence of a single non-axisymmetric roll for pure buoyancy flow in cylinders of $A = 1$ [8], [18], the distortion of the rotationally symmetric thermocapillary flow mode by the buoyancy-driven convection is almost imperceptible, even under 1g-conditions. Marangoni and buoyancy flow act in the same direction, when the configuration of Fig. 1 is heated from below and cooled from above. With a surprisingly weak interaction, the heat transfer rate is thus increased by only about 7% under earth-gravity (Fig. 9). On the other hand, surface tension and buoyancy forces counteract in a floating zone heated from above and cooled from below (Tab. 1). The steady-state average Nusselt number reduces by about 9% compared to 0-g conditions (Fig. 9). These results demonstrate that, for the given configuration, Marangoni convection is very dominant over natural convection, even under earth-gravity. This is in excellent agreement with experimental observations [16],[19] and numerical investigations [1], [3], [26].
In the initially isothermal case 2, the toroidal vortex gradually migrates from the bottom to the top (Fig. 8). The abrupt rise of the bottom temperature by $2\,\Delta T$ results in an increased heat transfer at the bottom. Although the transient development of the flow and temperature fields is very different from the one of case 1, the same steady-state heat transfer ($\overline{Nu} = 7.44$) is obtained, as the Marangoni number is the same for both cases. Moreover, the identity of the Nusselt numbers is a further indication that our numerical code works correctly. However, due to the temporary inactivity of the top disk, it takes more time to reach steady-state conditions in case 2.

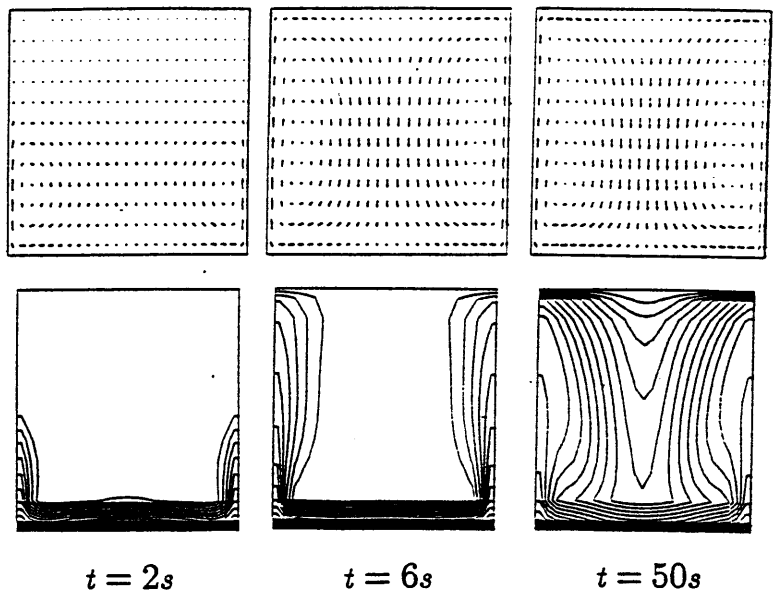

Figure 8: Transient development of velocity and temperature fields (Case 2, $Ma = 5000$, $Ra = 1.8 \cdot 10^4$, $Bo = 3.6$, $Pr = 1.92$)

For comparison purposes, pure buoyancy flow with $Ra = 1.8 \cdot 10^4$ has been simulated in a cylindrical enclosure with rigid walls under 1-g (Tab. 1). The corresponding Nusselt number amounts to only about 1/3 of the value for pure Marangoni flow. This ratio once more clearly demonstrates the dominance of thermocapillary flow in the liquid bridge considered.

The dependence of the heat transfer on the strength of the Marangoni convection already established in [11] has been extended up to $Ma = 10^7$ (Fig. 9). For Marangoni numbers $Ma \leq 200$, the Nusselt number does not deviate significantly from unity, which represents pure heat conduction. At higher Marangoni numbers, the velocities in the floating zone rise due to an increased driving force. For $Ma > 10^5$, a gradual decline in the heat transfer occurs, as the driving temperature gradients are reduced to a greater extent at high Marangoni numbers, as shown by Straub et al. [23], [25]. The displacement of the isotherms in Figs. 2 and 8 from the bulk towards the heated and cooled walls by Marangoni convection agrees qualitatively well with the experimental results of Preisser et al. [16] and Schwabe et al. [21].

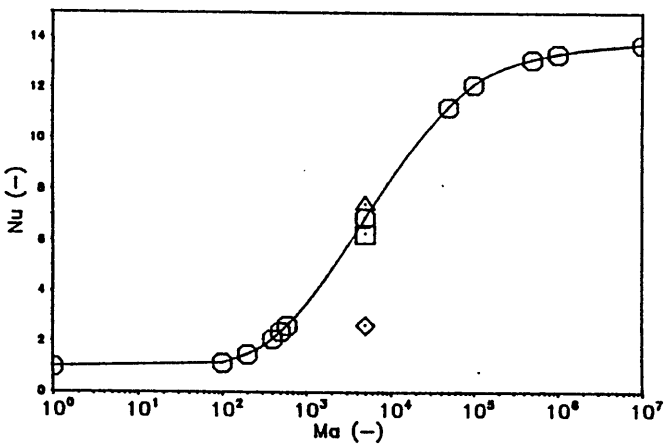

Figure 9: Overall heat transfer ($\overline{Nu}$) as a function of the strength of the thermocapillary convection (Ma) in a liquid bridge of $A = 1$ under micro-gravity

△ BC ↑ ↑ MC (1-g) ◇ pure BC (1-g)
□ BC ↑ ↓ MC (1-g) ⊙ pure MC (μ-g)

In numerous experiments [5]–[7], [9], [14], [16], [20]–[22] a transition from steady Marangoni convection to oscillatory flow has been observed, when a critical Marangoni number is exceeded. Besides, oscillations have also been obtained in the numerical calculations of Chang et al. [1] and Rupp et al. [17]. Although the range of the investigated Marangoni numbers has been extended to $1 \leq Ma \leq 10^7$ compared to a former study [11], only damped oscillations due to the transient nature of the phenomenon were observed (Fig. 10). No stable oscillations as in the experiments occurred. According to [18], the transient development of the flow can also be described by the maximum dimensionless velocity (Fig. 11), as it represents the upper limit for all fluid velocities. In Figs. 10 and 11 the transient behaviour of heat transfer and fluid flow is shown for $Ma = 500$, $Ma = 5000$, and $Ma = 50000$. It is obvious that the flow field changes more rapidly than the temperature field. Furthermore, a time-lag in the Nusselt numbers at the top and bottom disks, which vanishes in the steady-state, is observed. The time for reaching steady-state conditions and the frequency with which the oscillations are damped increase with the Marangoni number.

The physical mechanism inducing stable oscillations in floating zones is still not completely clarified. Chun [7] concludes that the oscillations are induced by waves of temperature perturbations travelling circumferentially around the free surface. Monti et al. [14] assume that the appearance of turbulence is, among others, the reason for the oscillations. By performing experiments under earth- and micro-gravity, Schwabe and his coworkers [21]

found that this form of instability is not due to a coupling of buoyancy and thermocapillary flow. Kamotani et al. [9] suggest that the S-shaped temperature profile along the free surface, also observed by Chun [6] and in this study (Fig. 6), together with its flexibility is responsible for the oscillations.

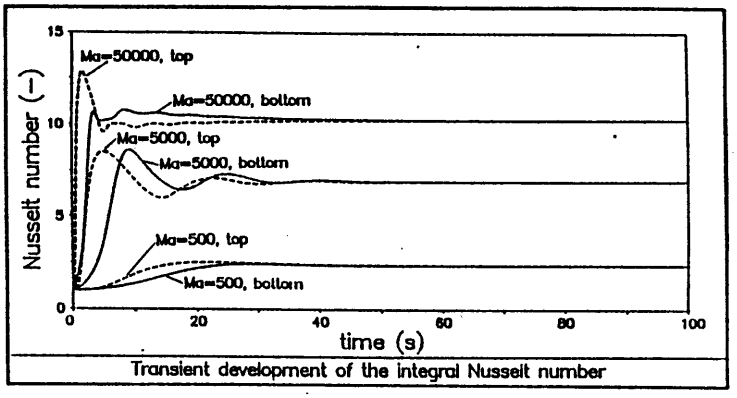

Figure 10: Transient behaviour of the integral Nusselt numbers at the bottom and top for three different Marangoni numbers

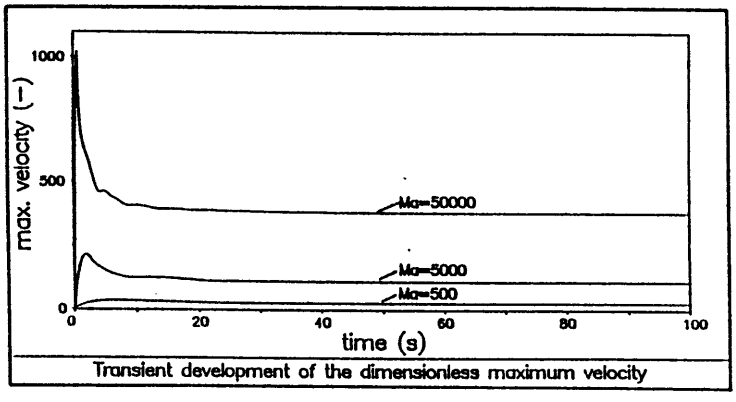

Figure 11: Dimensionless maximum velocity in the system as a function of time for three different Marangoni numbers

Chun and Wuest [5] assumed that the critical Marangoni number for the transition to oscillatory Marangoni convection depends on the aspect ratio A and the Prandtl number Pr. However, Kamotani et al. [9] showed that these two are not the only parameters to characterize the onset of oscillatory flow. An overview of critical Marangoni numbers in floating zones for different aspect ratios and Prandtl numbers, deduced both experimentally and theoretically, is given in Tab. 2. According to Preisser et al. [16], the critical Marangoni number is reduced by about 10%, when the free surface is thermally insulated. Although no relation in Tab. 2 is strictly valid for $Pr = 1.92$ and $A = 1$, it can be assumed that the critical Marangoni number is of the order 10^4 for the given configuration. In any case, the investigated range of Marangoni numbers includes the critical value. Despite several numerical modifications, no stable oscillations could be detected. More recently, Napolitano and Monti [15] performed space experiments, where no oscillations could be observed at $Ma \approx 4 \cdot 10^4$. They derived that the dynamic Weber number, and not the Marangoni number is the characteristic criterion for oscillations. However, since the physical mechanism of oscillatory Marangoni convection is not fully understood yet, further studies, both experimentally and numerically, are necessary.

Reference	Year	Fluid	Pr	A	Ma_c
[5]	1979	CH_3OH	6.8	0.73	$0.876 \lesssim Ma_c \lesssim 1.073 \cdot 10^4$ †
[20]	1979	$NaNO_3$	9.24	0.62	$Ma_c \approx 1.6 \cdot 10^4$
[21]	1982	$NaNO_3$	8.9	0.57	$Ma_c \approx 7 \cdot 10^3$
[16]	1983	$NaNO_3$	8.9	≤ 0.58	$Ma_c = 7.4 \pm 1.4 \cdot 10^3$
[17]	1989	theoret.	≥ 1	0.6	$Ma_c = 2884 \cdot Pr^{0.638}$
		Si, theoret.	0.02	0.6	$Ma_c = 300$
		GaAs, theoret.	0.068	0.6	$Ma_c = 1800$
[22]	1990	Si, extrapol.	0.03	0.5	$Ma_c \approx 90$
			≥ 1	0.5	$Ma_c \approx 1417 \cdot Pr^{0.716}$ ‡
		$NaNO_3$	7	$0.33 \leq A \leq 1.33$	$Ma_c \approx 555 \cdot A + 6670$ ‡
		$NaNO_3$	7	≥ 1.33	$Ma_c \approx 9836 \cdot A - 5704$ ‡

Table 2: Critical Marangoni numbers for floating zones

† In [5] the Marangoni number is calculated with the radius R, while here the height H is used.

‡ own correlations derived from data in [22]

List of symbols

a	thermal diffusivity	R	radius of the cylinder
A	aspect ratio	Ra	Rayleigh number
Bo	Bond number	t	time
c_p	isobaric specific heat capacity	T	temperature
D	diameter of the disk	$\vec{v}$	vector of velocity $= (v_r, v_\varphi, v_z)^{\mathrm{T}}$
g_z	axial gravitational acceleration	z	axial coordinate
H	zone height	β_p	volume coefficient of expansion
Ma	Marangoni number	ΔT	temperature increment ($\Delta T > 0$)
Nu	Nusselt number	η	dynamic viscosity
$\overline{Nu}$	average Nusselt number	ν	kinematic viscosity
p	pressure	ϱ	density
Pr	Prandtl number	φ	azimuthal coordinate
r	radial coordinate	σ	surface tension

subscripts:

c	critical value	φ	azimuthal component
r	radial component	0	reference value
z	axial component		

References

[1] Chang, Ch.E.; Wilcox, W.R., and Lefever, R.A.: *Thermocapillary Convection in Floating Zone Melting: Influence of Zone Geometry and Prandtl Number at Zero Gravity*, Mat. Res. Bull., vol. 14, pp. 527-536, 1979.

[2] Chun, Ch.H.: *Stroemungsvorgaenge in schwerelosen Schmelzzonen bei Anwesenheit elektromagnetischer Felder*, Scientific Report, BMFT-FB W 77–42, Hannover, 1977.

[3] Chun, Ch.H.: *Beitraege zur Marangoni-Konvektion in zylindrischen Schmelzzonen: Experimentelle Simulation und Berechnung des Einflusses der Erdschwere*, Scientific Report, BMFT-FB W 78–39, Hannover, 1978.

[4] Chun, Ch.H. and Wuest, W.: *A Micro-Gravity Simulation of Marangoni Convection*, Acta astronautica, vol. 5, no. 9, pp. 681-686, 1978.

[5] Chun, Ch.H. and Wuest, W.: *Experiments on the Transition from the Steady to the Oscillatory Marangoni-Convection of a Floating Zone under Reduced Gravity*, Acta astronautica, vol. 6, no. 9, pp. 1073-1082, 1979.

[6] Chun, Ch.H.: *Experiments on Steady and Oscillatory Temperature Distribution in a Floating Zone due to the Marangoni Convection*, Acta astronautica, vol. 7, nos. 4-5, pp. 479-488, 1980.

[7] Chun, Ch.H.: *Marangoni Convection in a Floating Zone under Reduced Gravity*, J. Crystal Growth, vol. 48, pp. 600-610, 1980.

[8] Crespo, E.; Bontoux, P.; Smutek, C.; Roux, B.; Hardin, G.; Sani, R., and Rosenberger, F.: *Three-Dimensional Simulations of Convection Regimes in Cylindrical Ampoules: Comparisons with Theoretical Analyses and Experiments*, Proc. 6th Europ. Sympos. Material Sciences under Microgravity Conditions – Bordeaux, France, ESA SP-256, pp. 529-537, Dec. 1986.

[9] Kamotani, Y.; Ostrach, S., and Vargas, M.: *Oscillatory Thermocapillary Convection in a Simulated Floating-Zone Configuration*, J. Crystal Growth, vol. 66, pp. 83-90, 1984.

[10] Kirchartz, K.-R.: *Numerische Simulation von Strukturaenderungen bei dreidimensionalen Konvektionsstroemungen*, Z. Flugwiss. Weltraumforsch., vol. 13, pp. 1-7, 1989.

[11] Marek, R. and Straub, J.: *Three-Dimensional Transient Simulation of Marangoni Flow in a Cylindrical Enclosure under Various Gravity Levels*, IUTAM Symposium on Microgravity Fluid Mechanics, Bremen, Germany, Sept. 1991. (An extended abstract of this study has been published in: Microgravity Science and Technology, vol. 4, no. 2, pp. 153-154, 1991.)

[12] Marek, R. and Straub, J.: *Hybridrelaxation – A Technique to Enhance the Rate of Convergence of Iterative Algorithms*, submitted to Numerical Heat Transfer, pt. B: Fundamentals, 1991.

[13] Mihelčić, M. and Wingerath, K.: *Instability of the Buoyancy Driven Convection in Si Melts During Czochralski Crystal Growth*, J. Crystal Growth, vol. 97, pp. 42-49, 1989.

[14] Monti, R.; Napolitano, L.G., and Mannara, G.: *Texus Flight Results on Convective Flows and Heat Transfer in Simulated Floating Zones*, Proc. 5th Europ. Sympos. Material Sciences under Microgravity Conditions – Schloss Elmau, ESA SP-222, pp. 229-236, 1984.

[15] Napolitano, L.G. and Monti, R.:*Surface Driven Flows: Recent Theoretical and Experimental Results*, Proc. 6th Europ. Sympos. Material Sciences under Microgravity Conditions – Bordeaux, France, ESA SP-256, pp. 551-555, Dec. 1986.

[16] Preisser, F.; Schwabe, D., and Scharmann, A.: *Steady and Oscillatory Thermocapillary Convection in Liquid Columns with Free Cylindrical Surface*, J. Fluid Mech., vol. 126, pp. 545-567, 1983.

[17] Rupp, R.; Mueller, G., and Neumann, G.: *Three-Dimensional Time Dependent Modelling of the Marangoni Convection in Zone Melting Configurations for GaAs*, J. Crystal Growth, vol. 97, pp. 34-41, 1989.

[18] Schneider, S. and Straub, J.: *Laminar Natural Convection in a Cylindrical Enclosure with Different End Temperatures*, submitted to Int. J. Heat Mass Transfer, 1991.

[19] Schwabe, D.; Scharmann, A.; Preisser, F., and Oeder, R.: *Experiments on Surface Tension Driven Flow in Floating Zone Melting*, J. Crystal Growth, vol. 43, pp. 305-312, 1978.

[20] Schwabe, D. and Scharmann, A.: *Some Evidence for the Existence of a Critical Marangoni Number for the Onset of Oscillatory Flow in Crystal Growth Melts*, J. Crystal Growth, vol. 46, pp. 125-131, 1979.

[21] Schwabe, D.; Preisser, F., and Scharmann, A.: *Verification of the Oscillatory State of Thermocapillary Convection in a Floating Zone under Low Gravity*, Acta astronautica, vol. 9, no. 4, pp. 265-273, 1982.

[22] Schwabe, D.; Velten, R., and Scharmann, A.: *The Instability of Surface Tension Driven Flow in Models for Floating Zones under Normal and Reduced Gravity*, J. Crystal Growth, vol. 99, pp. 1258-1264, 1990.

[23] Straub, J.; Weinzierl, A., and Zell, M.: *Thermokapillare Grenzflaechenkonvektion an Gasblasen in einem Temperaturgradientenfeld*, Thermo- and Fluid Dynamics, vol. 25, pp. 281-288, 1990.

[24] Straub, J. and Schneider, S.: *Transient Convection caused by Acceleration Disturbances*, IUTAM Symposium on Microgravity Fluid Mechanics, Bremen, Germany, Sept. 1991.

[25] Straub, J.; Betz, J., and Marek, R.: *Numerical Simulation of Marangoni Convection around Gas Bubbles in a Liquid Matrix*, presented at the 8th Europ. Sympos. Material Sciences under Microgravity Conditions, Brussels, Belgium, April 1992.

[26] Wilcox, W.R. and Chang, Ch.E.: *Analysis of Surface Tension Driven Flow in Floating Zone Melting*, Int. J. Heat Mass Transfer, vol. 19, pp. 355-366, 1976.